Mineralogy and Petrology (1995) 53: 1–26

Mineralogy and Petrology

Al-spinels in primitive arc volcanics

F. N. Della-Pasqua[1], V. S. Kamenetsky[1,2], M. Gasparon[1], A. J. Crawford[1], and R. Varne[1]

[1] Department of Geology, University of Tasmania, Hobart, Tasmania, Australia
[2] Vernadsky Institute of Geochemistry, Moscow, Russia

With 6 Figures

Received November 17, 1993;
accepted February 15, 1994

Summary

Al-rich spinels ($100Cr/(Cr + Al) < 5$, $Al_2O_3 > 50$ wt%) are common in alpine peridotites, both terrestrial and lunar mafic and ultramafic cumulates, and in certain metamorphic rocks, but they are apparently rare in terrestrial volcanic rocks. Here we describe the occurrence of Al-rich spinel inclusions in olivine phenocrysts in island arc volcanic rocks from five new localities: Bukit Mapas (Sumatra) and eastern Bali in the Sunda arc, and Epi, Merelava, and Ambrym islands in the Vanuatu arc. More commonly, relatively Cr-rich spinels also occur as inclusions in the same olivine phenocrysts, and it appears that the Cr-poor aluminous spinels must be in disequilibrium with the host basaltic melts. In the rocks studied, Al-rich spinels also coexist with trapped silicate glasses and highly aluminous clinopyroxene in melt inclusions in olivine. This paragenesis suggests an origin involving contamination by localised Al-rich melt pockets as opposed to a xenocrystic origin. Two mechanisms to produce this high-Al melt in basaltic magma chambers are suggested: (1) localized high-Al melt production by complete breakdown of assimilated lower crustal gabbroic rocks. In this model the high-Al melt may crystallise Al-rich spinels which are subsequently trapped as solid inclusions by phenocryst phases of the host basaltic melt or may be trapped as melt inclusions in which Al-rich spinels and Al-rich clinopyroxene crystallise as daughter phases, and (2) incongruent breakdown of amphibole in amphibole-rich cumulates in sub-arc, or sub-OIB volcano magma chambers. The latter reaction produces a melt with ~ 20–22% of Al_2O_3, aluminous clinopyroxene, Al-rich spinel and olivine. Mixing between these amphibole breakdown products and host basaltic melt may occur throughout the evolution of a magmatic system, but particularly during recharge with hot magnesian basalt batches. Aluminous spinels and aluminous clinopyroxene produced during amphibole breakdown, or perhaps crystallised from aluminous melt produced in the same reaction, are incorporated into the magma during recharge, and subsequently trapped, together with the coexisting Cr-spinels, by crystallising olivine and clinopyroxene.

Zusammenfassung

Al-Spinelle in primitiven Inselbogen-Vulkaniten

Al-reiche Spinelle ($100Cr/(Cr + Al) < 5$, $Al_2O_3 > 50$ Gew.%) sind in alpinen Peridotiten, in terrestrischen und lunaren mafischen und ultramafischen Kumulaten und in manchen metamorphen Gesteinen weit verbreitet, aber sie scheinen in terrestrischen, vulkanischen Gesteinen selten zu sein. Wir beschreiben hier das Vorkommen von Al-reichen Spinell-Inklusionen in Olivinkristallen von Inselbogen-Vulkaniten von 5 neuen Lokalitäten: Bukit Mapas (Sumatra) und Ost-Bali im Sunda-Bogen und die Inseln Epi, Merelava und Ambrym im Vanuatu-Bogen. Relativ Cr-reiche Spinelle kommen häufiger auch als Einschlüsse in denselben Olivin-Kristallen vor, und es scheint, daß Chrom-arme Aluminiumspinelle im Ungleichgewicht mit ihren basaltischen Mutterschmelzen stehen. In den untersuchten Gesteinen kommen Al-reiche Spinelle zusammen mit Silikatgläsern und Aluminium-reichen Klinopyroxenen in Schmelzeinschlüssen in Olivinen vor. Diese Assoziation weist auf einen Ursprung hin, der Kontamination durch lokalisierte Al-reiche "pockets" von Schmelze involviert; dies steht im Gegensatz zu einem Ursprung als Xenokristalle. Wir schlagen zwei Mechanismen vor, die diese Aluminium-reiche Schmelze in basaltischen Magmakammern erzeugen können: (1) lokalisierte Produktion von Aluminium-reicher Schmelze durch vollkommene Auflösung von assimilierten gabbroischen Gesteinen aus der unteren Kruste. In diesem Modell kann die Aluminium-reiche Schmelze Al-reiche Spinelle kristallisieren, die dann anschließend als feste Einschlüsse von Phenokristallen in der basaltischen Mutterschmelze eingefangen werden oder als Schmelzeinschlüsse, in denen Al-reiche Spinelle und Al-reiche Klinopyroxene als Tochterphasen kristallisieren. (2) Inkongruenter Zerfall von Amphibol in Amphibol-reichen Kumulaten in Magmakammern unter Inselbögen oder unter OIB-Vulkanen. Die letztgenannte Reaktion erzeugt eine Schmelze mit ungefähr 20–22% Al_2O_3, Aluminium-haltigen Klinopyroxen, Al-reichen Spinell und Olivin. Mischung zwischen diesen Produkten des Zerfalls von Amphibol und basaltischer Mutterschmelze kann während der ganzen Evolution eines magmatischen Systems stattfinden, aber besonders während der Zufuhr neuer heißer Magnesium-reicher Basalte. Aluminium-haltige Spinelle und Klinopyroxene, die während des Zerfalls von Amphibol entstanden sind oder vielleicht aus einer Aluminium-haltigen Schmelze in derselben Reaktion produziert wurden, werden während der Neuzufuhr in das Magma inkorporiert und im Anschluß daran, zusammen mit den koexistierenden Cr-Spinellen, von kristallisierendem Olivin und Klinopyroxen eingefangen.

Introduction

Minerals of the spinel group (hereafter called spinel) are important accessory phases in virtually all intrusive and volcanic crustal rocks. The almost ubiquitous occurrence of spinel in peridotite xenoliths and alpine peridotites indicates that this mineral is also widespread in the upper mantle. Understanding of the compositional variation, thermodynamic properties and paragenesis of spinels is important for three reasons: (1) spinels occur in rocks of very different composition ranging from mantle peridotites to granites, and can be used to classify and characterise a very large variety of rock types (*Irvine*, 1965; *Dick* and *Bullen*, 1984; *Arai*, 1987, 1992); (2) spinel crystallizes simultaneously with liquidus silicates (eg. olivine, orthopyroxene), and remains on the liquidus until the complete solidification of the rock; and (3), spinel is an extensive solid solution of cations with different valence, and its composition reflects that of the parent melt and conditions of crystallisation (e.g. *Dick* and *Bullen*, 1984; *Sack* and *Ghiorso*, 1991).

Cr-rich spinel (Cr_2O_3 in the range 15–70 wt%) is the most common spinel in ultramafic and basaltic volcanic rocks, but Al-rich and Cr-poor ($Cr_2O_3 < 5$ wt%) pleonaste, belonging to the $Mg(Fe^{3+}Al)_2O_4$–$Fe(AlFe^{3+})_2O_4$ series is rare in volcanic assemblages. To the best of our knowledge, Al-rich spinels in arc lavas are previously reported from only four localities: in basanitoids of Grenada (*Arculus*, 1974, 1978; *Arculus* and *Wills*, 1980) and Guadeloupe (*Bissainte* et al., 1993) in the Lesser Antilles, in high-Al primitive basalts from Akutan Island (Hot Springs Bay Volcanics) in the Aleutian arc (*Romick* et al., 1990), and in cognate cumulate gabbroic inclusions dredged from Epi caldera, Vanuatu (*Crawford* et al., 1988). *Arculus* (1978) suggested that Al-rich spinels in volcanics might be xenocrysts derived from disaggregated granulites and lherzolite nodules.

An alternative origin that might be considered is crystallization from anomalously Al-rich magmas. Strikingly Al-poor and Cr-rich spinels in boninites from Cape Vogel (Papua New Guinea) (*Walker* and *Cameron*, 1983) and Howqua (Victoria) (*Crawford*, 1980) are considered to have crystallized from unusual melt compositions with extremely low Al content (*Crawford*, 1980). Conversely, one could consider that the existence of Cr-poor, Al-rich spinels in other volcanic rocks might reflect an abnormally high Al_2O_3 content in the melt.

Here we describe the occurrence of high-Al spinels coexisting with Cr-spinels as inclusions in phenocrysts in arc lavas from five new localities: Bukit Mapas (Sumatra) and Bali in the Sunda arc, and Epi, Ambrym and Merelava islands in the Vanuatu arc. Consideration of factors which lead to crystallisation of magmatic Al-rich spinel may provide an insight into the origin and significance of high-Al melts. Moreover, the coexistence of both Al-rich and Cr-rich spinels strongly suggests that contamination and mixing may be significant magmatic processes in the petrogenesis of the host rocks.

The Al-spinel bearing samples

Cr-spinel is the dominant oxide phase in all samples in this study, and occurs as inclusions in olivine phenocrysts. The Al-rich spinels are relatively minor and were found included in olivine phenocrysts: in ankaramitic lavas of Bali, western Epi, and Merelava; in basaltic lavas of Ambrym; in basaltic andesites of Bukit Mapas; and also in clinopyroxene phenocrysts in the Bali ankaramites. No Cr-spinels or Al-spinels were found as phenocrysts. Whole-rock compositions are shown in Table 1. Except for Bukit Mapas basaltic andesites, the petrography and geochemistry of all other host lavas has been previously studied (see below, and Table 2).

Vanuatu Arc

Epi (samples: 71041, 71046) Pleistocene ankaramitic lavas from western Epi include some of the most primitive and Ca-rich compositions in the Vanuatu arc (*Barsdell* and *Berry*, 1990). The lavas consist dominantly of clinopyroxene [$Mg/(Mg + Fe_{tot})$] hereafter $Mg\# = 77$-94) and olivine (Fo_{93-68}) phenocrysts.

Ambrym (sample: 74583) This sample is an olivine + clinopyroxene-phyric tholeiitic lava with restricted forsterite content (Fo_{94-90}) for the majority of the olivine phenocryst population (*Eggins*, 1989).

Table 1. *Representative whole-rock analyses. (1) Barsdell and Berry (1990), (2) Eggins (1989), (3) Barsdell (1988), (4) Wheller (1986), (5) Gasparon (1993)*

Location	Western Epi	Western Epi	Ambrym	Merelava	Bali	Bukit Mapas
Sample #	71046	71041	74583	31541	67424	SMG166
	(1)	(1)	(2)	(3)	(4)	(5)
SiO_2	48.20	47.80	51.45	50.82	46.44	55.00
TiO_2	0.39	0.43	0.70	0.64	0.56	0.70
Al_2O_3	11.50	13.60	14.71	13.67	9.12	16.27
$Fe_2O_{3\,tot}$	9.90	10.60	10.68	9.25	11.45	7.62
MnO	0.16	0.18	0.18	0.21	0.20	0.15
MgO	13.50	10.70	9.16	9.74	17.48	5.49
CaO	14.40	14.20	10.08	12.90	11.78	9.19
Na_2O	1.05	1.29	2.55	1.89	1.22	2.81
K_2O	0.31	0.35	1.09	0.38	0.61	1.91
P_2O_5	0.07	0.09	0.21	0.12	0.21	0.19
L.O.I.	0.10	0.31	−0.41	0.20	0.41	0.39
H_2O					0.37	
Rest					0.33	
total	99.58	99.55	100.40	99.82	100.18	99.72
Cr (ppm)	820	448	—	372	1055	—

Merelava (sample: 31541) The detailed geochemistry and petrogenesis of these primitive olivine (Fo_{92-68}) + clinopyroxene (Mg# = 93-75)-phyric ankaramitic lavas is described in *Barsdell* (1988).

Sunda Arc

Bali (sample: 67424) The high-K shoshonitic ankaramites of southeastern Bali are the oldest, and compositionally, the most distinctive lavas in Bali (Table 1), constituting part of the Ulakan Formation (*Wheller*, 1986). The Bali ankaramites consist dominantly of clinopyroxene (Mg# = 67-92) and olivine (Fo_{92-77}) phenocrysts, but rare plagioclase phenocrysts are also present.

Olivine and clinopyroxene phenocrysts in all ankaramitic samples described above are euhedral to subhedral in shape and show only minor resorption. Compositional variations in these phenocrysts reflect differentiation trends and are not indicative of magma mixing.

Bukit Mapas (South Sumatra, Sample: SMG 161–166) Bukit Mapas is a basaltic andesite central volcano in the South Sumatra Province (*van Bemmelen*, 1949), Pleistocene or younger in age. Samples are olivine-phyric lavas with rare rounded, resorbed quartz xenocrysts, clinopyroxene phenocrysts, and microphenocrysts of olivine, pyroxene, plagioclase and amphibole. All petrographic, mineral chemical and whole-rock data for Bukit Mapas are from *Gasparon* (1993). A small subset of representative analyses from Bukit Mapas is shown here.

Description and types of Al-spinel inclusions

Mineral inclusions in olivine phenocrysts are red-brown Cr-spinel, clinopyroxene, and green Al-rich spinels and range up to about 200 μm across. Melt inclusions vary from glassy to crystalline, sometimes with optically distinct daughter phases (spinel, clinopyroxene) and interstitial glass and shrinkage bubbles. Fluid inclusions are common in all samples, and rare sulphide globules up to 60 μm across were found only in Bukit Mapas olivines.

Petrographically, two types of Al-rich spinel crystals are recognized. Type 1 includes Al-rich spinels occurring as discrete crystalline inclusions, and type 2 includes Al-rich spinel crystals in melt inclusions in olivine (or rarely, clinopyroxene) phenocrysts. Relative to Cr-spinel solid inclusions, the proportion of Al-rich spinel solid inclusions is small, as they are found in only approximately 1% of phenocrysts examined. Type 2 is abundant in Bukit Mapas basaltic andesites, less common in western Epi ankaramites, and rare at all other localities (see Table 2).

Type-1 Solid Inclusions

Al-rich spinels are dull green, euhedral to sub-rounded crystals ≤ 100 μm across. Importantly, they may coexist in the same host grain with inclusions of Cr-spinel. Their distribution within host phenocrysts is highly variable. They may occur as individual grains, or as clusters of two to several tens of grains, usually randomly distributed, or both. Occasionally, both Cr-spinel and Al-rich spinel inclusions may form a regular zoning pattern that follows relic crystal-melt interfaces (Fig. 1E).

Table 2. *Summary of occurrence and frequency of aluminous spinels. (1) Frequency is given relative to the abundance of Cr-spinel solid inclusions for Al-spinel solid inclusions and relative to the abundance of primary melt inclusions without Al-spinels for melt inclusions with the assemblage Al-spinel + Al-clinopyroxene + Al-glass, (rare $\approx$ 1/100 and common $\approx$ 1/20). The distribution of inclusions within their host showed zoning patterns in Western Epi, Bali, and Bukit Mapas olivines and clinopyroxenes*

Location	host phenocryst	Al-spinel inclusion type and frequency[1]	
		as solid inclusions	in melt inclusions
		(Type-1)	(Type-2)
Indonesian arc			
Bali	olivine	rare	rare
	clinopyroxene	none found	very rare
Bukit Mapas	olivine	rare	very common
Vanuatu arc			
Ambrym	olivine	rare	none found
Merelava	olivine	none found	rare
	clinopyroxene	none found	none found
Western Epi	olivine	rare	common
	clinopyroxene	none found	none found

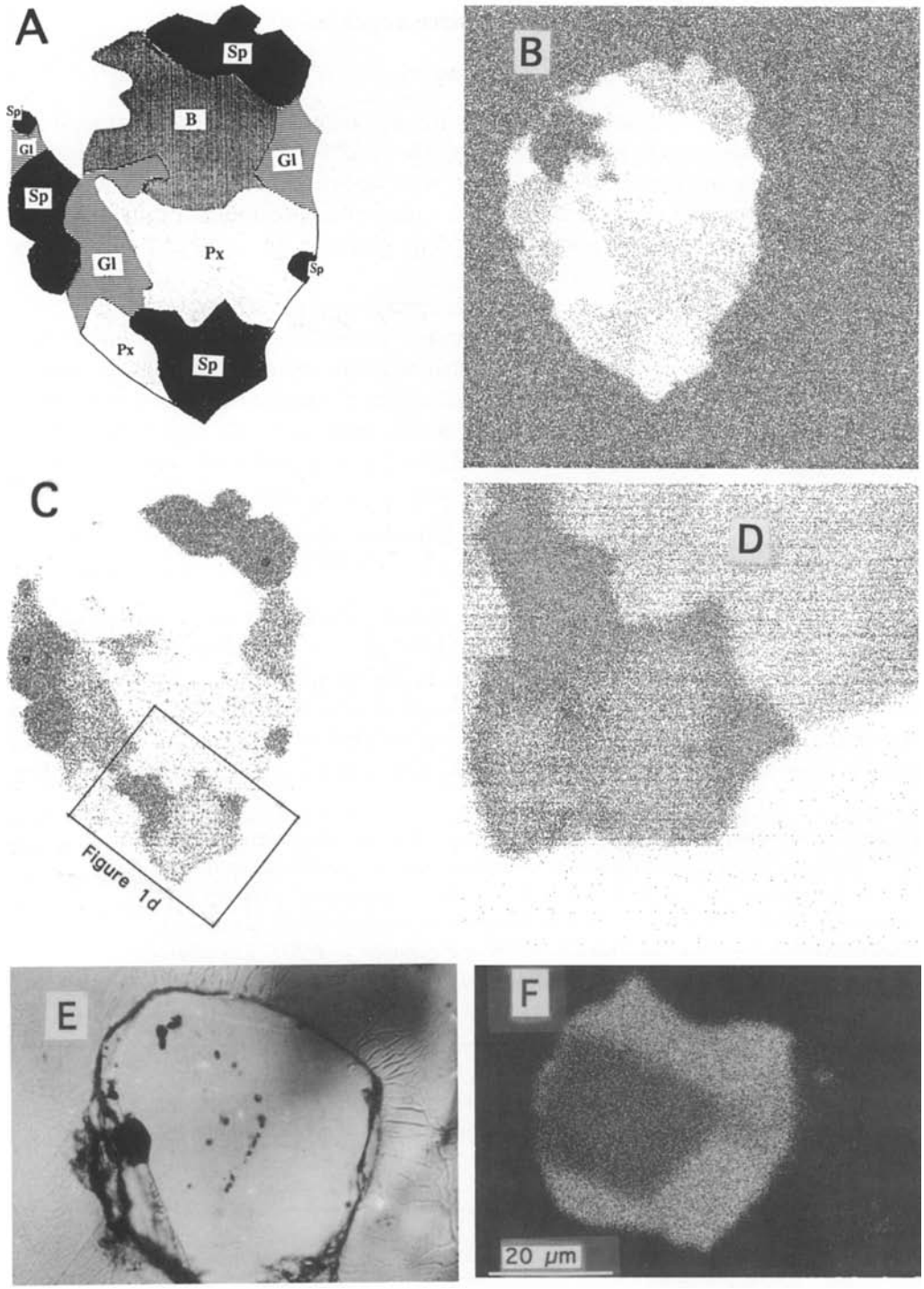

Fig. 1. Al-spinels in melt inclusions (Type-2) are associated with clinopyroxene daughter crystals and a residual glass. Figure 1A shows this typical daughter phase assemblage (Al-rich spinel + Al-rich Cpx + residual glass). Width of melt inclusion approximately 80 μm across. Host phenocryst is olivine. *Sp* Al-rich spinel, *Px* Al-rich clinopyroxene, *Gl* residual glass after the crystallisation of daughter phases, *B* Vapour phase cavity. Figure 1B–D X-ray distribution maps (CAMECA SX 50); Fig. C, D, and F, Al Ka; Fig. 1B Mg-Ka. Figure 1D: Enlarged inset of Fig. 1C. Note overgrowth of daughter Al-rich spinel on Cr-spinel. Cr-spinel was trapped simultaneously with melt by the host olivine. 1E: Zoning pattern produced by Al-rich spinel inclusions and Al-rich spinel bearing melt inclusions in olivine. 1F: Electron microprobe scanned image (Al_2O_3). Note overgrowth of Al-rich spinel on Cr-spinel solid inclusion. Host phenocryst is olivine

Al-rich spinel rims on Cr-spinels were found in western Epi and in Bukit Mapas (Fig. 1F) and are similar to those described in metamorphosed mafic-ultramafic rocks from the Panton sill (Western Australia) by *Hamlyn* (1975), and in high-K arc picrites from Ringgit-Besser, Java (*Kamenetsky* and *Varne*, unpubl. data). We note also that in some samples, solid inclusions have adjacent to them a small portion of melt that appears to have been trapped together with the solid spinel inclusion. This feature is observed for both Cr-spinels and Al-rich spinel solid inclusions. These polyphase inclusions are easily distinguished from melt inclusions of type 2 by their absence of clinopyroxene crystals, and the relative volume proportions of spinel and melt.

Type-2 Melt Inclusions

Most olivine phenocrysts contain primary crystalline melt inclusions composed of fluid, crystal, and residual, interstitial glass phases. Clinopyroxene is the dominant daughter crystal phase in crystalline melt inclusions and olivine has nucleated on the melt inclusion wall. Glassy melt inclusions and polyphase melt inclusions with trapped Cr-spinels are also present. Melt inclusions range in size up to a few hundred μm, usually with euhedral shapes, less commonly elongated or irregular. Melt inclusions with Al-rich spinels however, are rare and tend to be surrounded by trails of small inclusions < 1 μm in size. These small inclusions broadly contour the outlines of the melt inclusion wall and remain equidistant from it, forming a corona inclusion surface that partially encloses the melt inclusion.

When present in melt inclusions, Al-rich spinels occur as individual crystals or as overgrowths on Cr-spinels which were also simultaneously trapped with the melt inclusion. Al-spinels in melt inclusions are always associated with clinopyroxene crystals and an interstitial glass (Fig. 1A–D). This association is always present and the assemblage Al-spinel + Al-clinopyroxene + glass is consistently found in all Al-spinel bearing melt inclusions.

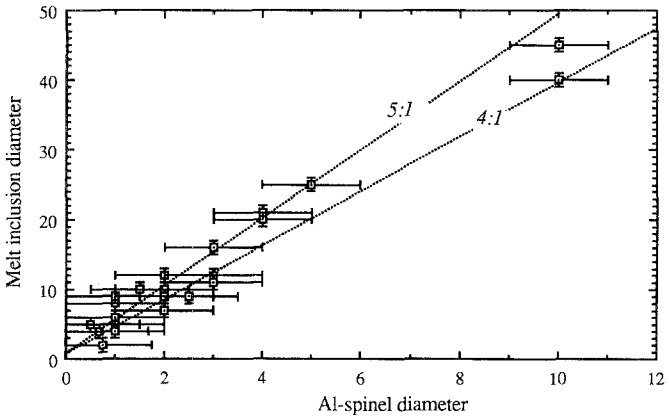

Fig. 2. The volume-proportion that Al-spinel occupies with respect to its host melt inclusion may be estimated from the value of the melt inclusion/Al-spinel diameter ratio. The slope indicates that Al-rich spinels occupy about 1–5 volume %. Arbitrary microscope units are used (1 unit $\approx$ 2 μm)

Clinopyroxene is the dominant phase in olivine-hosted Al-spinel bearing melt inclusions, occupying approximately 40–60% of the melt inclusion volume commonly found as a single crystal. These clinopyroxenes differ texturally from those found in crystalline melt inclusions, which grow forming numerous clinopyroxene crystals. Al-rich spinel is a minor phase in these melt inclusions. Diameters of coexisting Al-rich spinel—melt inclusion pairs from western Epi samples are plotted in Fig. 2 and correspond to ratios of 1 : 4 to 1 : 5, indicating that Al-rich spinel occupies approximately 1–5% of the melt inclusion volume. Similar Al-rich green spinels are also reported in melt inclusion assemblages in clinopyroxene phenocrysts in Mt. Etna alkalic lavas (*Frezzotti* et al., 1991).

Whole-rock and mineral chemistry

Analytical techniques

Several samples from each volcanic unit were hand-crushed, sieved, and their phenocrysts (olivine-clinopyroxene) hand-picked from size fractions 0.3–0.5 mm. The grains were mounted in epoxy, polished to expose inclusions and analysed using a fully automated three spectrometer Cameca SX 50 electron microprobe (University of Tasmania) calibrated with natural mineral standards (PAP data reduction). Olivine (USNM 111312/444), basaltic glasses (USNM 111240/52, UTASGLASS 498), clinopyroxene (USNM 122142; *Jarosewich* et al., 1980), and spinel (UV 126, *Lavrentev* et al., 1974); USNM 117075 New Caledonia Cr-spinel) were used as standards. Analytical conditions were 15 kV accelerating voltage, 20 nA (minerals) and 10 nA (glasses) beam current, and 1–2 μm (minerals) and 10–20 μm (glasses) beam size. Inclusions were analysed as pairs together with their coexisting host (within 20–30 μm distance). Spinel analyses were recalculated assuming a stoichiometric composition (*Finger*, 1972).

Olivine-hosted melt inclusions containing Al-spinels from Bukit Mapas and Bali were partly homogenised using the heating-stage technique with visual control, described by *Sobolev* et al. (1980). Melt inclusions were progressively heated to approximately 1250 °C to melt crystalline daughter phases for 15–20 minutes and then quenched to a glass prior to analyses.

Analytical results

Representative analyses of spinel and associated phases in melt inclusions, and of Al-rich spinel inclusions, are given in Tables 3 and 4 respectively, and are shown in Figure 3, 4 and 5. The following key points are noted:

1. Spinels show a wide range in Cr/(Cr + Al) (herein Cr#), varying from Cr-rich, Al-poor to Cr-poor, Al-rich (Fig. 3A). This range may be subdivided into three intervals: Cr-rich spinels (Cr# > 50), Cr-poor spinels (Cr# < 5) and Cr–Al spinels of intermediate compositions (Cr# 5–50), corresponding respectively to Al_2O_3 contents of approximately <20 wt%, >50 wt%, and 20–50 wt%.
2. Both Al-rich and Cr-rich spinels occur in olivines that span similar compositional ranges (Fo_{92-75}) and have the same range of NiO values (0.05–0.40 wt %) (Fig. 3F). The strong positive correlation between Fo content of the host olivine and Mg# in the spinel (Fig. 3E) is most likely due to the fact that both types of spinel have re-equilibrated with host olivine.

Table 3. *Representative analyses of Al-spinel and Cr-spinel solid inclusions. WE: Western Epi, MER: Merelava, BAL: Bali, BM: Bukit Mapas, AM: Ambrym. (#) Numbers in italics are compositions of Al-rich spinel borders enclosing Cr-spinel crystals*

	Al-Spinels										
Location	WE	WE	WE	WE	WE	WE	BAL		BAL		AM
Sample #	*71041*	*71041*	*71041*	*71041*	*71041*	*71041*	*67424*		*67424*		*74583*
TiO_2	0.26	0.67	0.25	0.16	0.23	0.48	0.56	*0.97*	0.47	*0.04*	0.25
Al_2O_3	45.80	51.88	56.04	51.06	55.74	43.75	10.95	*38.59*	9.67	*64.88*	56.56
Cr_2O_3	6.76	4.87	1.18	11.01	0.50	7.65	48.84	*23.51*	48.07	*0.44*	0.08
Fe_2O_3	17.03	11.70	13.22	8.31	12.71	16.92	11.27	*6.60*	13.26	*3.40*	12.44
FeO	14.09	12.62	9.56	9.81	13.53	16.86	18.22	*15.17*	20.76	*9.64*	7.59
MgO	16.55	18.22	20.61	19.74	18.00	14.40	10.19	*15.44*	8.42	*21.01*	21.35
MnO	0.05	0.13	0.05	0.14	0.13	0.23	0.33	*0.15*	0.42	*0.14*	0.10
NiO	0.13	0.20	0.17	0.16	0.10	0.13	0.17	*0.29*	0.15	*0.27*	0.13
ZnO	0.09	0.11	0.18	0.13	0.09	0.24	0.09	*0.09*	0.20	*0.25*	0.10
Total	100.84	100.48	101.33	100.58	101.14	100.73	100.64	*100.88*	101.47	*100.14*	98.60
Mg# host olv.	83.8	85.0	87.5	88.3	85.2	82.0	84.5	*88.1*	86.9	*85.6*	92.2
Mg#spl(Fe^{2+})	67.7	72.0	79.4	78.2	70.3	60.3	49.9	*64.5*	79.5	*42.0*	83.4
Cr#	9.0	5.9	1.4	12.6	0.6	10.5	74.9	*29.0*	0.5	*76.9*	0.1

(continued)

Table 3 (*continued*)

	Al-Spinels								Cr-Spinels				
Location	BM	BM	BM	BM		BM	BM		WE	BAL	AM	BM	MER
Sample #	*166*	*166*	*166*	*166*		*166*	*166*		*71041*	*67424*	*74583*	*166*	*31541*
TiO_2	0.16	0.33	0.60	0.46	*0.35*	0.43	0.69	0.23	0.25	0.51	0.31	0.43	0.25
Al_2O_3	62.90	56.11	57.27	46.29	*54.63*	39.43	19.02	*57.60*	8.52	9.70	6.88	12.74	9.75
Cr_2O_3	0.25	0.46	0.59	9.05	*1.27*	14.93	35.80	*0.22*	56.18	48.25	60.06	51.02	47.73
Fe_2O_3	2.61	12.66	10.52	13.16	*12.50*	14.42	16.42	*13.01*	7.62	12.26	5.80	7.50	13.85
FeO	13.39	11.32	11.41	13.16	*11.90*	14.80	16.56	*9.19*	16.01	18.66	12.67	14.94	18.57
MgO	18.10	19.30	19.40	16.85	*18.57*	15.33	12.31	*20.94*	11.26	9.66	13.16	12.38	9.56
MnO	0.11	0.08	0.17	0.17	*0.06*	0.14	0.31	*0.15*	0.34	0.17	0.20	0.10	0.52
NiO	0.00	0.17	0.14	0.12	*0.14*	0.20	0.00	*0.25*	0.12	0.03	0.08	0.08	0.03
ZnO	0.17	0.12	0.18	0.17	*0.16*		0.15	*0.05*	0.00	0.09	0.00	0.09	0.02
Total	97.69	100.55	100.29	99.42	*99.58*	99.69	101.25	*101.64*	100.30	99.33	99.16	99.28	100.28
Mg# host olv.	86.9	83.9	84.5	85.3	*85.3*	85.5	88.5	88.5	89.3	87.7	93.4	89.3	85.9
Mg#spl(Fe^{2+})	70.7	75.2	75.2	69.5	*73.6*	64.9	57.0	*80.3*	55.6	48.0	64.9	59.6	47.8
Cr#	0.3	0.5	0.7	11.6	*1.5*	20.3	55.8	*0.3*	81.6	76.9	85.4	72.9	76.6

Table 4. *Representative analyses of mineral phases in melt inclusions, abbreviations as shown in Table 3. Some difficulty was encountered in analysing small crystals in melt inclusions, particularly the interstitial glass. Small beam size accounts for the high totals in some of the analysis. * Indicates phases present but too small to analyse. # Numbers in italics are compositions of Al-rich spinels enclosing Cr-spinel crystals. " No clinopyroxene crystals present perhaps due to its crystallisation on inclusion walls*

Location	WE	WE	WE	WE	WE	WE	WE	BAL	BAL	MER	BM	BM	BM	BM	BM	BM	BM		BM	
Sample #	*71046*	*71046*	*71041*	*71041*	*71041*	*71041*	*71041*	*67422*	*67424*	*31541*	*161*	*161*	*161*	*161*	*161*	*161*	*'161*		*'161*	
HOST PHASE	*Olv.*	*Olv.*	*Olv.*	*Olv.*	*Olv.*	*Olv.*	*Olv.*	*Olv.*	*Cpx.*	*Olv.*	*Olv.*	*Olv.*	*Olv.*	*Olv.*	*Olv.*	*Olv.*	*Olv.*		*Olv.*	
Mg# host	82.7	83.7	84.4	76.6	85.7	85.1	84.2	89.1	85.1	84.0	86.9	86.6	86.2	86.9	83.9	90.4	87.4		91.0	
SPINEL																	core	rim(#)	core	rim(#)
TiO_2	0.18	0.10	0.19	1.22	0.24	0.13	0.20	0.09	0.18	*	*	0.40	0.38	0.16	0.27	0.22	0.74	*0.52*	0.38	*0.17*
Al_2O_3	57.75	60.86	60.59	51.22	58.86	62.78	61.05	67.44	48.70			57.48	57.76	62.90	55.60	50.63	16.18	*58.80*	14.75	*61.63*
Cr_2O_3	1.94	0.06	0.42	0.52	0.07	0.16	0.36	0.12	3.71			0.07	0.93	0.25	1.35	0.30	35.72	*0.03*	48.00	*0.16*
MgO	17.61	19.15	18.34	12.45	18.40	18.21	17.73	20.87	17.89			20.00	20.70	18.10	18.96	18.11	10.76	*19.61*	12.92	*22.61*
MnO	0.14	0.14	0.12	0.12	0.08	0.11	0.12	0.08	10.43			0.07	--	0.11	0.18	0.05	0.25	*0.16*	0.11	*0.07*
Fe_2O_3	8.43	7.31	7.42	11.87	6.85	2.37	6.52	—	18.78			11.14	10.88	3.46	13.72	10.78	17.99	*10.09*	8.54	*6.96*
FeO	14.27	11.93	13.48	21.59	12.32	13.31	14.89	9.61	0.46			10.52	9.53	13.78	12.17	8.38	18.15	*11.48*	14.22	*6.10*
NiO	0.15	0.20	0.21	0.09	0.17	0.12	0.22	0.16	0.17			0.13	0.15	—	0.19	0.29	0.00	*0.13*	0.16	*0.42*
ZnO	0.19	0.35	0.14	0.24	0.04	0.08	0.10	0.26	0.19			0.02	0.19	0.17	0.19	0.10	0.12	*0.23*	0.10	*0.07*
Total	100.65	100.10	100.92	99.33	97.03	97.26	101.19	98.62	100.51			99.83	100.52	98.94	102.62	88.86	99.91	101.05	99.18	98.19
Mg# (Fe^{2+})	68.7	74.1	70.8	50.7	72.7	70.9	68.0	79.5	76.2			77.2	79.5	70.1	73.5	79.4	51.4	75.3	61.8	*86.9*
Cr#	2.2	0.1	0.5	0.7	0.1	0.2	0.4	0.1	4.86			0.1	1.1	0.3	1.6	0.4	59.7	0.0	68.6	*0.2*
PYROXENE																				
SiO_2	41.21	41.67	46.40	42.71	45.28	42.70	45.86	53.21	"	52.96	39.22	43.88	50.09	40.18	40.82	45.92	45.25		46.19	
TiO_2	1.66	1.04	0.68	2.92	0.58	0.76	0.91	0.45		0.18	1.78	1.89	0.52	1.78	1.98	1.12	1.38		1.35	
Al_2O_3	14.91	13.35	10.23	12.21	8.68	12.65	20.11	1.78		5.10	13.46	10.87	4.65	13.46	14.57	9.94	9.05		10.27	
Cr_2O_3	0.00	0.03	0.00	0.04	0.06	0.00	0.01	0.46		0.34	0.04	0.01	0.61	0.04	0.06	0.04	0.06		0.02	
MgO	10.14	10.35	13.09	10.93	13.29	10.83	6.67	17.95		14.74	11.68	12.62	16.24	11.79	10.42	13.10	13.20		13.51	
CaO	21.90	21.88	21.87	21.13	23.38	22.54	18.71	22.65		20.23	20.73	21.04	21.95	20.73	21.97	22.82	21.88		22.87	
MnO	0.13	0.05	0.14	0.19	0.15	0.08	0.11	0.15		0.13	0.07	0.12	0.09	0.07	0.06	—	0.11		0.03	
FeO	3.01	2.76	3.55	4.47	0.15	2.37	7.50	2.12		5.38	0.00	2.81	2.00	0.38	2.61	2.13	7.06		5.51	
Fe_2O_3	7.09	8.92	6.41	5.24	8.95	9.42	—	1.52		—	13.18	5.56	3.74	12.09	7.26	4.70	—		--	
Na_2O	0.32	0.32	0.23	0.54	0.16	0.24	0.97	0.16		0.76	0.35	0.39	0.26	0.35	0.26	0.26	—		0.36	
Total	100.39	100.37	102.58	100.35	100.68	101.59	100.85	100.45		99.81	100.50	99.18	100.16	100.87	100.01	100.03	97.99		100.11	
Mg# (Fe_{tot})	65.9	63.1	71.5	68.0	74.3	64.1	61.4	90.2		83.0	63.7	74.3	84.4	65.2	67.1	78.6	74.0		81.4	
GLASS																				
SiO_2	61.64	62.12	62.51	64.22	65.61	62.96	54.28	*	61.38	65.41	57.40	56.89	*	57.40	*	*	57.47		60.18	
TiO_2	0.59	0.24	0.39	0.71	0.43	0.46	0.49		0.68	0.26	0.28	0.76		0.28			0.71		0.29	
Al_2O_3	19.62	25.60	23.98	23.59	24.56	22.01	21.97		16.45	23.82	26.29	24.95		26.29			25.22		26.06	
Cr_2O_3	0.06	0.04		—	0.03	0.12			0.01	—	0.06	0.01		—			0.01		0.06	
MgO	3.28	2.45	0.72	0.38	0.33	1.63	3.43		3.00	0.68	0.91	0.66		0.91			0.56		0.90	
CaO	6.16	1.01	3.92	2.69	2.36	4.71	10.58		6.39	3.63	1.08	1.90		1.08			1.52		1.84	
MnO	--	—	—	—	—	—	0.05		—	—	0.04	--		0.04			0.00		0.00	
FeO	2.86	3.14	1.67	1.55	1.15	1.62	4.67		2.39	1.32	1.17	1.62		1.17			1.38		0.92	
NaO	3.99	3.33	6.05	3.21	3.06	5.42	4.07		3.87	5.64	12.96	10.52		12.96			11.55		5.36	
K_2O	1.56	2.55	2.45	2.93	3.03	2.19	1.21		3.80	1.56	0.99	2.04		0.99			1.71		3.53	
P_2O_5	0.38	0.34	0.44	0.48	0.49	0.40	0.33		0.21	0.26	0.87	1.08		0.85			0.94		0.39	
Total	100.14	100.82	102.12	99.76	101.05	101.52	101.07		98.17	102.58	102.04	100.42		101.97			101.07		99.52	

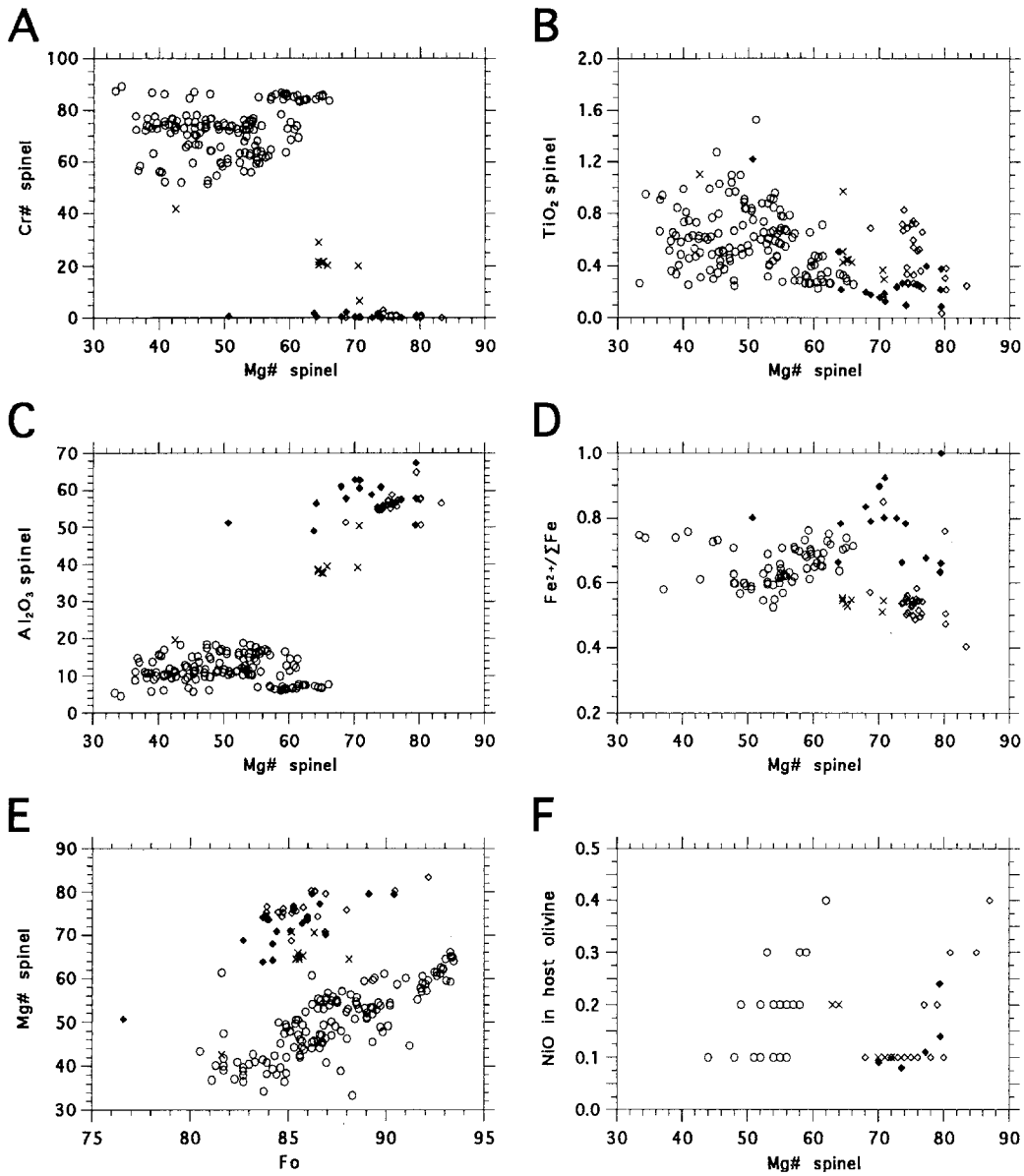

Fig. 3. Spinel inclusions in olivine phenocrysts. Figure 3A–E includes spinels from all localities studied in this paper (Bali, Sumatra, Epi, Ambryn, Merelava). Figure 3F includes spinel composition from Bukit Mapas only. *Circles:* Cr-spinels (Cr# = >50), *diamonds:* Al-spinels (Cr# < 5), *crosses*: intermediate compositions (Cr# = 5–50). Filled symbols represent compositions of spinel crystals in melt inclusions included in olivine, open symbols represent compositions of discrete spinels included in olivine phenocrysts

3. The majority of Al-rich spinels have lower $Fe^{2+}/\sum Fe$ values compared to coexisting Cr-rich spinel (Fig. 3D), and within each group (Al-rich spinel and Cr-rich spinel) there is a broad inverse correlation between Mg# and TiO_2, typical of crystal fractionation (eg. Bukit Mapas, Fig. 3F).
4. Al-spinels in melt inclusions (type 2) have higher Mg# compared to discrete spinel inclusions (Type-1), and have restricted Cr# compositions (Cr# < 5), whereas discrete spinel crystals show a wide range in Cr# (0–90), (Fig. 3A and 4).

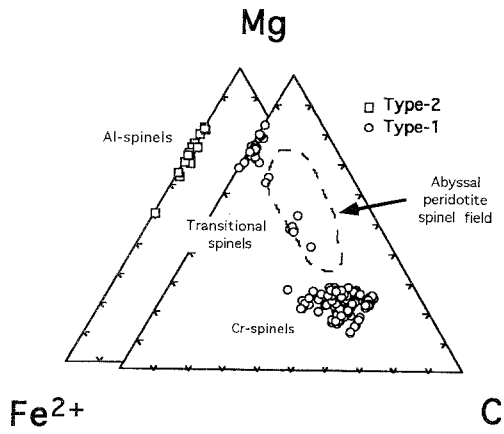

Fig. 4. Spinel compositions in: melt inclusions (Type-2) and solid inclusions (Type-1) in olivine. Compositional range of spinels in abyssal peridotites from *Dick* and *Bullen* (1984). Note the compositional overlap between high Al-spinels in melt and solid inclusions

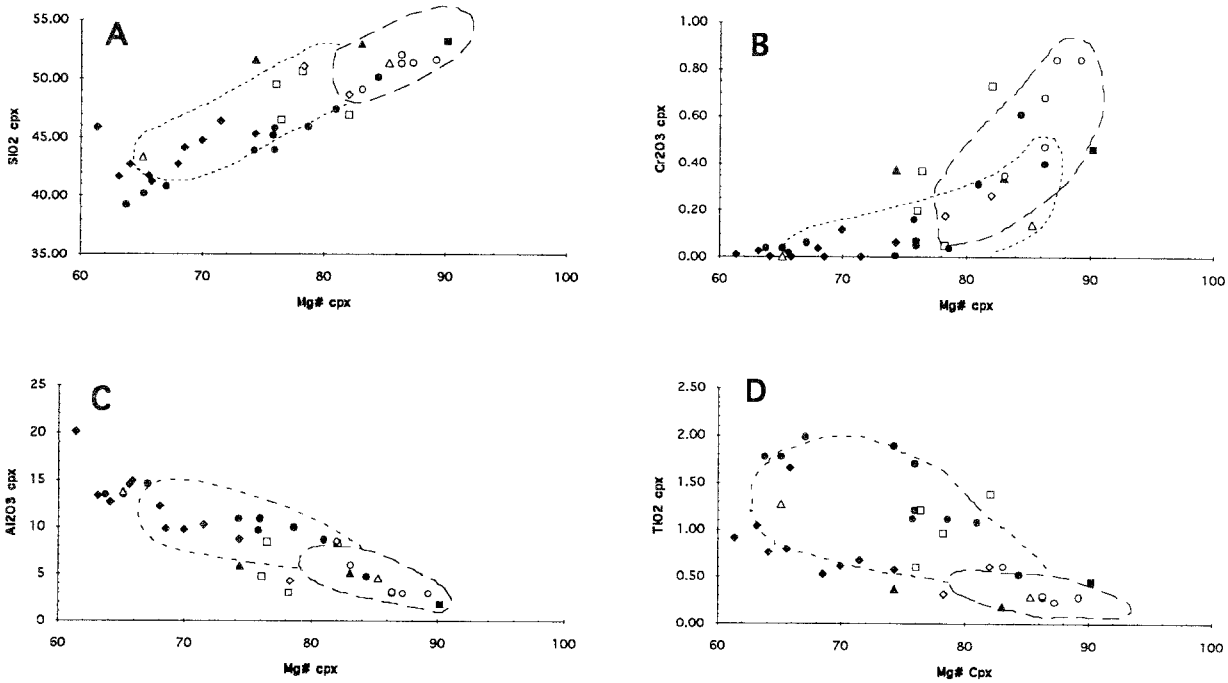

Fig. 5a–d. Composition of clinopyroxene inclusions in olivine. Open symbols represent compositions of clinopyroxene included in olivine, filled symbols represent composition of clinopyroxene crystals in melt inclusions included in olivine. Symbol shapes as in Fig. 3. *Broken lines*: composition field of clinopyroxene phenocrysts (all localities in this study). *Dotted line*: compositional field of clinopyroxenes found in association with Al-rich spinels in volcanic rocks (data compiled from *Arculus*, 1978, and *Romick* et al., 1990)

5. Clinopyroxene inclusions in olivine, both as discrete inclusions and crystals in melt inclusions, have a very wide compositional range, with exceptionally high Al_2O_3 contents (up to 20 wt%, Fig. 5c), and SiO_2 contents as low as 38 wt% (Fig. 5a) being not uncommon. Discrete clinopyroxene inclusions tend to be more aluminous than clinopyroxene phenocrysts (Fig. 5C). We note that the compositions of clinopyroxenes coexisting with Al-rich spinels in melt inclusions are similar to clinopyroxene compositions reported by *Arculus* (1978) in Grenada

Table 5 **A.** *Composition of melt inclusions in olivine phenocrysts from Bukit Mapas and Bali. The homogenisation of melt inclusions with Al-rich spinel, Al-rich clinopyroxene, and residual Si-rich Al-rich glass assemblages was only partially achieved as Al-rich spinel and vapour phases persisted even to high temperatures. Average compositions of partially homogenised melt inclusions and average compositions of Al-rich spinels are shown in column (1) and (2) respectively. Melt compositions, calculated by mass balance, after the addition of 1 volume % (column 3) and 5 volume % (column 4) of Al-rich spinel, are Al-rich and compare with Al-rich melt composition indicated in Fig. 6 and with aluminous compositions of lower crust aluminous gabbros. Melt inclusion composition of parent basaltic melt in olivine ($Fo_{91.7}$), from* Della Pasqua and Varne, *(in prep).*

B *Lower crustal gabbroic compositions, 6 = average of mafic inclusions representing the composition of lower crust, Northeast Honshu arc, Japan (*Kushiro, *1990, Table 3), (7) = average composition of accreted lower crust gabbroic rocks, Talkeetna arc, southeastern Alaska (*Pearcy *et al., 1990, Table 1), (8) = average composition of gabbroic pegmatoids from Marum Ophiolite Complex, Northern Papua New Guinea (*Jaques *et al., 1983, Table 1)*

A	Average composition of two partially homogenized melt inclusions with Al-spinel (1)	Average composition of Al-spinel in melt inclusions (2)	Partially homogenised melt inclusions with added Al-spinel 1 vol. % added (3)	5 vol. % added (4)	Composition of melt inclusion without Al-spinel (5)
Bukit Mapas (Sunda arc)					
SiO_2	44.50		43.72	41.15	
TiO_2	1.11	0.39	1.10	1.06	
Al_2O_3	16.29	56.48	16.87	19.29	
Cr_2O_3			0.00	0.00	
FeO	8.37	20.28	8.53	9.26	
MgO	9.56	19.62	9.69	10.31	
CaO	16.76		16.46	15.50	
MnO	0.07	0.08	0.07	0.07	
NaO	2.79		2.74	2.58	
K_2O	0.62		0.61	0.57	
P_2O_5	0.22		0.22	0.20	
total	100.29	96.85	100.00	100.00	
Bali (Sunda arc)					
SiO_2	45.84	0.13	45.15	42.45	44.43
TiO_2	0.73	0.31	0.72	0.70	0.78
Al_2O_3	17.94	58.70	18.57	21.01	11.08
Cr_2O_3	0.07	0.49	0.07	0.10	0.10
FeO	9.48	21.53	9.67	10.39	10.30
MgO	7.15	17.24	7.31	7.91	16.20
CaO	15.82		15.57	14.64	13.44
MnO	0.17	0.12	0.17	0.17	0.07
NaO	2.10		2.06	1.94	1.93
K_2O	0.59		0.58	0.55	1.31
P_2O_5	0.14		0.13	0.12	0.35
total	100.01	98.84	100.00	100.00	99.99

(continued)

Table 5 (*continued*)

B	*Average composition of crustal gabbros* (6)	(7)	(8)
SiO_2	42.39	43.78	41.53
TiO_2	1.01	0.68	0.36
Al_2O_3	20.01	18.69	22.11
FeO	10.89	10.17	10.48
MgO	10.54	10.63	5.85
CaO	12.92	13.97	14.62
MnO	0.16	0.17	0.17
NaO	1.65	1.74	0.68
K_2O	0.24	0.11	0.20
P_2O_5	0.19	0.08	0.01
total	100.00	100.02	96.01

basanites that also carry Al-spinels. Moreover, *Romick* et al. (1990) and *Bissainte* et al. (1993) described Al-rich spinel phenocrysts coexisting with aluminous clinopyroxenes quite similar to those described here.

Additional observations include:

1. Compositions of interstitial glasses in melt inclusions associated with Al-rich spinel and aluminous clinopyroxenes are characterised by high SiO_2 (to 65 wt%) and high Al_2O_3 (to 26 wt%) contents (Table 4). They are residual after the crystallisation of spinel, olivine and clinopyroxene. Compositionally, these felsic glasses are similar to residual glasses in melt inclusions reported from Mount Etna nodules (*Frezzotti* et al., 1991).
2. Al-rich spinel in melt inclusions did not melt during heating experiments. Recalculated compositions of partly homogenised melt inclusions in olivine from Bukit Mapas and Bali (Table 5A) are characterised by low SiO_2 and high Al_2O_3 contents.

Discussion

Possible models for the origin of Al-spinels

A number of possibilities for the origin of the Al-rich spinel in these arc lavas might be put forward:

1. A xenocrystal origin. Accidental trapping and/or assimilation of material containing the Al-rich spinel crystals (e.g. granulite or lherzolite xenoliths) by host magmas has been suggested by *Arculus* (1978) and *Kuehner* et al. (1981) as a possible origin for high-Al spinels in some volcanic rocks. Descriptions of Al-rich spinel-bearing xenoliths and individual xenocrysts and megacrysts include examples from the alkaline lavas of Iki Island, Japan (*Aoki*, 1968), the Kerguelen archipelago (*Talbot* et al., 1963), New South Wales (*Binns*, 1969; *Binns* et al., 1970), Mt. Melbourne Volcanic Field (Antarctica) (*Horning* and *Wörner*, 1992), and Hawaiian tholeiites (*Sen* and *Leeman*, 1991). However, the Cr-poor compositions of our Al-rich spinel inclusions are markedly different from the more Cr-rich spinels in peridotites ($Cr\# > 10$, *Dick*

and *Bullen*, 1984; *Dick* and *Fisher*, 1984), and no other phases or relics of metamorphic or ultramafic assemblages were observed. Furthermore, the distribution of crystalline inclusions occasionally follows the crystallographic shape of the host olivine, denoting relic crystal-melt interfaces where spinel nucleated on growing olivine crystals; therefore, Al-rich spinels were present in the melt and probably crystallising with forsteritic olivine (Fo_{92-75}). This strongly supports the trapping of these discrete high-Al inclusions during magmatic crystallisation of olivine, and is thus generally inconsistent with a xenocrystic origin.

2. Formation of Al-rich spinel via breakdown (and/or exsolution) of Al-bearing minerals in the magma chamber, followed by their subsequent trapping by crystallising olivines and clinopyroxenes. In this model, the formation of Al-rich spinel is explained as the result of solid state reactions, mainly due to decreasing pressure and consequent exsolution or breakdown of high-pressure Al-bearing phases. Examples include spinel exsolution from aluminous pyroxene (*Obata*, 1980; *Aoki* and *Shiba*, 1973; *Varne*, 1978), from plagioclase (*Wiebe*, 1986; *Wass*, 1973; *Wilkinson*, 1975) and from leucite (*Jaques* and *Foley*, 1985), or breakdown of biotite (*Venturelli* et al., 1984), garnet (*Griffin* et al., 1984; *Aoki* and *Prinz*, 1974; *Neal* and *Nixon*, 1985; *Reid* and *Dawson*, 1972) and Ti-magnetite (*Prince* and *Putnis*, 1979). Exsolution reactions are easily recognised in thin section, but none were observed in the samples studied, and an origin for the Al-rich spinels involving exsolution from a higher-pressure aluminous phase can be confidently excluded. Besides being texturally obvious, breakdown reactions (e.g. of biotite, garnet or FeTi oxides) produce Cr-free spinels that reflect the composition of the precursor phase, and are unlikely to produce the Cr# compositional range observed in Type-1 spinels.

3. Crystallisation of Al-rich spinel (and other phases) at high pressures, followed by their trapping at lower pressures by olivine and clinopyroxene. Kushiro and *Yoder* (1966) studied the peritectic reaction Fo + Al-diopside + Al-enstatite + Al-spinel at 8–9 kbar, and their results are often cited to support the formation of Al-rich spinel at high pressure. Various authors have proposed that the rather aluminous Al–Cr spinels in mid-ocean ridge basalts (MORB) may have originated by crystallisation at relatively high pressure (e.g. *Irvine*, 1967; *Sigurdsson* and *Schilling*, 1976; *Dick* and *Bryan*, 1978; *Fisk* and *Bence*, 1980). There is limited experimental support for this hypothesis (*Green* et al., 1972; *Råheim* and *Green*, 1974; *Falloon* and *Green*, 1987; *Delano*, 1980; *Bartels* et al., 1991; *Thy*, 1991; *Johnston* and *Draper*, 1992), although we are aware of no convincing experimental demonstration of the pressure dependence of Al partitioning in spinel. Rather, *Dick* and *Bullen* (1984) suggest that this pressure effect on the composition of spinel is largely due to variations in the partition coefficient for Cr, resulting in a lower Cr# in the spinel at high pressures.

One main line of evidence argues against the applicability of a high pressure origin for the Al-rich spinels found in our arc lavas: Al-rich spinel rims were found on typical Cr-spinel crystals in both (1) discrete spinel inclusions and (2) spinel in melt inclusions, (ie. Cr-spinel preceded Al-spinel).

4. Formation of Al-rich spinel as a result of closed system breakdown of phases which were previously trapped by magmatic olivine, e.g. amphibole. Several experimental studies have focused on the decompression breakdown of pargasite (*Lykins* and *Jenkins*, 1992; *Holloway*, 1973). Textural evidence of such reactions, and the forma-

tion of Cr–Al spinel, Al-rich glass, Al-rich clinopyroxene and high-Mg olivine as breakdown products have been documented in the olivine-orthopyroxene matrix of lherzolite nodules from alkaline basalts of the Newer Volcanic Province in Victoria (*Yaxley* et al., 1991; and our unpubl. data). It is therefore tempting to consider a mechanism by which pargasitic amphibole is included by olivine and clinopyroxene at high pressures, and subsequently broken down (during ascent) to produce the Al-rich spinel + Al-rich clinopyroxene + Al-rich glass assemblages observed in melt inclusions. However, it is unlikely that pargasite would crystallize (or survive) in a basaltic magma capable of crystallizing Fo_{92} olivine (T probably > 1200 °C). It also demands that at least some of the pargasite breakdown occurred outside of 'armouring' olivine host crystals, since some discrete inclusions of Al-rich spinel are included in olivines in each of the studied samples without associated Al-rich pyroxene or melt. Any Al-spinels produced by pargasite breakdown within a basaltic magma might either be dissolved, or overgrown by rims of typical near-liquidus high-Cr spinel. In fact, we occasionally observe the opposite, with high-Cr spinels rimmed by green Al-rich spinel.

5. Crystallisation of Al-rich spinel from a discrete high-Al melt in the magma chamber. Co-crystallisation of both Cr-rich and Al-rich spinels from the same melt is highly unlikely (e.g. *Maurel* and *Maurel*, 1982; *Sack* and *Ghiorso*, 1991; *Nielsen* and *Dungan*, 1983). Furthermore, zoning from Cr-rich cores to Al-rich rims on many spinels from each of our localities argues against co-crystallization from a homogeneous melt. The rather sparse amount of Al-spinel compared with Cr-spinel in these (and most other) arc basalts suggests that the favourable conditions for crystallisation of Al-rich spinel were restricted in space, and probably in time. The occurrence of Al-rich spinel with intermediate compositions toward Cr–Al spinel is strong evidence for the mixing of melts which were parental to normal Cr-spinels, and to Al-rich spinel.

Both Cr-spinel and Al-rich spinel show a strong correlation between their Mg# and Fo value of their host olivine (Fig. 3E). Such a relationship is indicative of equilibrium between associated olivine and spinel (*Sigurdsson*, 1977).

We now focus on evidence supporting a magmatic origin for the Al-spinel. Important facts supporting a magmatic origin for these Al-rich spinels include:

— their association with magmatic olivine, with which they have equilibrated (Fig. 3E), and occasionally with magmatic Cr-spinel;
— they have euhedral crystallographic shapes in melt inclusions, and are euhedral to sub-rounded as discrete spinel inclusions in olivine;
— they are aligned along the host olivine growth outlines;
— they sometimes occur as rims on Cr-spinel crystals (and never *vice versa*), in both solid inclusions and melt inclusions, reflecting the temporal sequence of crystallisation;
— they commonly crystallised together with particularly Al-rich pyroxene as daughter crystals inside melt inclusions, leading to the formation of a residual felsic Al-rich glass, and to the formation of a shrinkage bubble. This consistent presence of Al-rich spinels, Al-rich clinopyroxene and Al-rich glass in melt inclusions cannot be coincidental and must reflect the crystallisation of these phases from an Al-rich, compositionally distinct trapped melt.

Constraints on the chemistry of the parent magmas of Al-spinels

Experimental studies of spinel-melt equilibrium (*Maurel* and *Maurel*, 1982, 1983) show that the Al content of spinel increases with Al concentration in the melt. Although these experiments were carried out with relatively low-Al melt compositions and at atmospheric pressure, an extrapolation of their correlation (Fig. 6) suggests that Al_2O_3 contents of melts in equilibrium with our Al-rich spinels may have been 20–22%.

Correlations between Al content in spinel and Al concentration in host rocks and glasses observed by *Sigurdsson* and *Schilling* (1976), *Crawford* (1980), *Dick* and *Bullen* (1984) and *Allan* et al. (1988) also support our assertion that it is possible to produce Al-rich spinel by crystallisation of a melt with exceptionally high Al_2O_3 content. Independent confirmation of this bulk composition control on the Al content of spinel comes from findings of Al-rich spinel in high-Al metamorphic rocks in association with other high-Al phases, such as staurolite, garnet, sapphirine, corundum, micas, and plagioclase (*Graham*, 1987; *Droop* and *Bucher-Nurminen*, 1984; *Grapes*, 1986), and in cumulates from hypothetical aluminous mantle melts

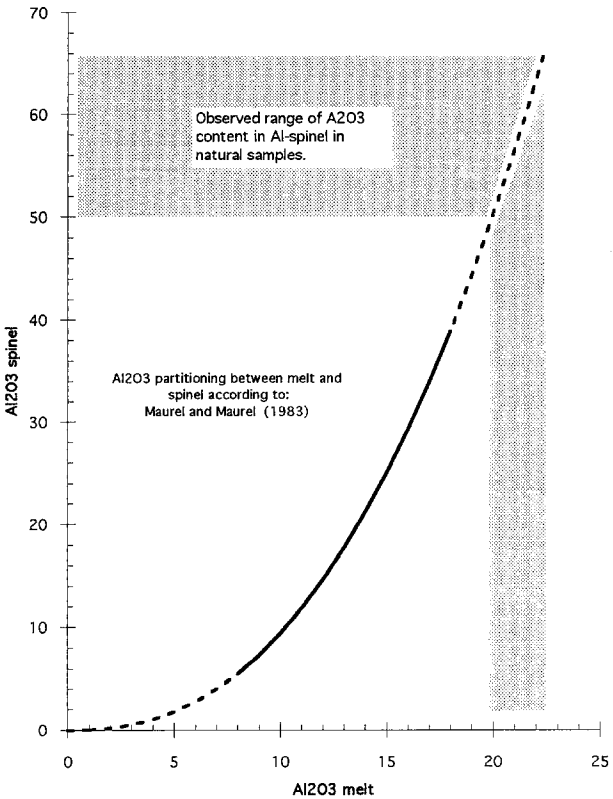

Fig. 6. Correlation between Al content in the melt and in spinel, according to *Maurel* and *Maurel* (1982). The dashed line is an extrapolation into the field of high-Al melts based on the partitioning of Al_2O_3 between Cr-spinel and silicate melt after *Maurel* and *Maurel* (1983, equation-2), for an Fe_2O_3 content in spinel of 5 wt%. Shaded area represents the compositional range of Al-rich spinels (Al_2O_3 > 50 wt%) found in this study. The extrapolation suggests that Al-rich spinels might have been in equilibrium with melts with Al_2O_3 contents of approximately 20–22 wt%

(*Nixon* et al., 1978; *Exley* and *Smith*, 1983). They also occur in highly aluminous lunar samples (e g. *Drever* et al., 1972; *Roeder* and *Weiblen*, 1972; *Haggerty*, 1972; *Reid*, 1972; *Reid* et al., 1972; *Cameron* et al., 1973; *Keil* et al., 1970). However, the latter differ significantly from terrestrial basalts in that they crystallised under reducing conditions. Such conditions significantly influence the Cr and Fe^{3+} partitioning, allowing more Al into octahedral sites (*Roeder* and *Reynolds*, 1991; *Schreiber* and *Haskin*, 1976; *Nielsen* and *Dungan*, 1983). Reducing crystallization conditions for lunar basalts are reflected in lower Fe^{3+} contents of their spinels, unlike Al-rich spinels described here which show higher Fe^{3+}/Fe^{2+} contents compared to coexisting Cr-spinels (Fig. 3D).

We have estimated the melt compositions in equilibrium with our Al-rich spinels by recalculating compositions of partially homogenised melt inclusions in olivines from Bukit Mapas and Bali (Table 5A, column 3 and 4) by addition of Al-spinel according to its estimated volume proportion in melt inclusions (1–5 vol.%) from Fig. 2. The recalculated melt compositions (Table 5B) have unusually low-Si and high-Al compositions (Si/Al < 2.2) that resemble those of lower crustal mafic xenoliths from northeastern Honshu (*Kushiro*, 1987, 1990), Tonsina, Alaska (*Pearcy* et al., 1990), and gabbros from the Marum ophiolites, Papua New Guinea (*Jaques* et al., 1983). According to *Dick* and *Bullen* (1984), low Si/Al melt compositions are capable of crystallizing Al-rich, Cr-poor spinel. Furthermore, low silica melt compositions can also favour the crystallisation of Al-rich, Si-poor pyroxenes (*Kushiro*, 1960). The association of Al-rich clinopyroxene with Al-rich spinel as phenocrysts and as cumulates has been observed in Lesser Antilles and Aleutians basalts (*Arculus*, 1978; *Romick* et al., 1990), and must therefore reflect peculiar melt compositions and crystallisation conditions.

Models for the generation of high-Al parent melts

We suggest, therefore, that one model for the origin of the high-Al spinels in the lavas we have studied is that they crystallized from local melt pockets with unusually low-Si and high-Al compositions, similar to compositions of aluminous gabbros in the lower crust. Assimilation and complete breakdown of lower crust gabbros may lead to the formation of local pockets of highly aluminous melts within the otherwise typical basaltic magma, and to crystallisation of Al-rich spinels. The composition of this host basaltic melt in Bali is shown in Table-5 column 5. Compositions of melt inclusions without Al-spinels are also shown for Merelava, Epi, Bali and Lombok in *Della-Pasqua* and *Varne* (in prep.) as part of a separate melt inclusion study aimed at establishing the composition of primary melts for these ankaramite suites. Olivine, and less frequently clinopyroxene phenocrysts, may subsequently trap both: a) Al-rich spinels as discrete inclusions and b) the melt from which Al-spinel and Al-clinopyroxene assemblages crystallised. The products of the crystallisation of basaltic melt and contaminant Al-melt, as well as the products of the crystallisation of mixed melts, are reflected in the wide Cr # compositional range of spinels. A good example of this may be the recent discovery of Al-rich green spinels in a tholeiitic picrite from Iceland (*I. Sigurdsson*, pers. comm., 1993). Emplacement of a hot, plume-related picritic magma beneath and through a MORB-related cumulate pile may lead to localized melting of the cumulates, and production of aluminous spinels.

If the above model is correct, it would be reasonable to suggest that Al-rich spinels should occur in any magmatic system where gabbroic cumulates and regular recharge of fresh magma batches are involved. Given their aluminous nature, early-crystallizing plagioclase and plagioclase-rich cumulate sequences, and open-system magma chambers, MORB might be the ideal candidates to crystallize Al-spinel via this mechanism. However, we have very carefully examined more than ten representative MORB suites, and have not recorded a single crystal of Al-spinel. Some further ingredient appears to be necessary to crystallize Al-spinel together with Cr-spinel from basaltic magmas.

All the terrestrial volcanic-cumulate suites that we are aware of that crystallised Al-rich spinel are either:

— alkaline intraplate basalt suites and their cumulates, including Balleny Is. (*Green*, 1992), Jan Mayen Is. (*Imsland*, 1980), Mt. Etna (*Frezzotti* et al., 1991) Papua New Guinea (our unpubl. data), Kerguelen (*Talbot* et al., 1963), tholeiitic picrites of Iceland (*I. Sigurdsson*, pers. comm.), and intraplate basalts in eastern Australia (*Binns* et al., 1970; *Wass*, 1973; *Wilkinson*, 1973, 1975; *Yim*, 1990) and China (*Fan* and *Hooper*, 1989),
— arc lavas or their cumulates [e.g. this study; *Aoki* (1968), *Arculus* (1978), *Arculus* and *Wills* (1980), *Snoke* et al. (1981), *Bissainte* et al. (1993), *Crawford* et al. (1988), *DeBari* and *Coleman* (1989); *DeBari* et al. (1987), Java (our unpubl. data)],
— ultrapotassic kimberlite-lamproite series rocks from many localities (e.g. *Jaques* and *Foley*, 1985; *Venturelli* et al., 1984; *Kuehner* et al., 1981; *Mazzone* and *Haggerty*, 1986; *Wagner* and *Velde*, 1987; *Exsey* and *Smith*, 1983; *Nixon* et al., 1978; *Pasteris*, 1983; *Kay* et al., 1983; *Reid* et al., 1975).

Relative to MORB, each of these magma series is relatively hydrous, and should be capable of crystallizing amphibole in near-solidus conditions. We have noted above that pargasite breaks down incongruently to form a very aluminous glass, aluminous clinopyroxene, Al-rich spinel and olivine. A second hypothesis for origin of these Al-rich spinels is therefore, that amphibole in amphibole-rich cumulates on the walls of magma chambers breaks down as a result of influx of hot magnesian parental basaltic magma. The strongly aluminous melts produced might form a sheath between the relatively unfractionated core basalt and the floor- and sidewall cumulate pile. Convective mixing associated with recharge of the magma chamber will provide the opportunity for trapping of this aluminous melt, and its crystallization products (Al-rich spinel and aluminous clinopyroxene). Olivine produced in the breakdown reaction will rapidly re-equilibrate with the fresh hot basaltic melt, but similarly-produced aluminous clinopyroxene may dissolve. Our attempts to melt Al-spinel hosted in melt inclusions show that it is difficult to dissolve, so that Al-rich spinel produced during amphibole breakdown may actually persist; the subrounded discrete Al-rich spinel inclusions in many olivine phenocrysts may reflect this process.

Whichever model is the correct one, and there may be several others that we have not considered here, a key ingredient must be a mechanism capable of producing a highly aluminous melt in a magmatic system frequented by magnesian basaltic magmas. We believe that the occurrence of green, Al-rich spinels in arc and intraplate basalts is more widespread than commonly believed. The mechanism required to generate suitable parental highly aluminous melts within a basaltic

magmatic system is not yet well understood, but its very existence demonstrates that we still do not have a thorough understanding of the evolution and dynamics of basaltic magmatic systems. Further studies will hopefully refine our models for the production and preservation of high-Al spinels in arc and intraplate basalts.

Conclusions

We have described coexisting Cr–Al spinels and Al-rich spinels inclusions in olivine and rare clinopyroxene phenocrysts in basalts and basaltic andesites from five arc volcanic suites. Petrographic and compositional features of both spinel groups indicate that they grew via magmatic crystallization, and that they are not simply xenocrysts derived from disaggregated lower crustal granulites. In partly crystallized former melt inclusions in olivine phenocrysts in these rocks, the occurrence of the Al-rich spinels together with particularly aluminous (commonly around 15% Al_2O_3) clinopyroxenes and very Al-rich residual glass indicates the presence of a highly aluminous (20–25% Al_2O_3) melt at some stage during the fractionation history of the host basalts. Any mechanism for the origin of the Al-rich spinels must be directly linked to a model capable of producing a highly aluminous melt in a basaltic magma chamber.

We consider two scenarios for the formation of high Al melts. The first involves digestion of gabbroic lower crustal xenoliths by the host magma, producing localized pockets of highly aluminous melt. A problem with this model is that green Al-rich spinels are unknown from MORB, whereas the composition and magmatic systems for MORB should optimize the chance for Al-rich spinel to crystallize. As an alternative, we note that all occurrences of green, Al-rich spinels in volcanic rocks of which we are aware occur in hydrous basaltic magmas, either arc-related, or intraplate in origin. We suggest that amphibole-rich sidewall cumulates in basaltic magmas chambers of these magmatic systems may melt incongruently during recharge with hot basaltic magma. This breakdown reaction produces a very aluminous melt, aluminous clinopyroxene, olivine, and Al-rich spinel. These breakdown products are then available for interaction with, and incorporation into, freshly injected batches of hotter, more primitive basalt.

Acknowledgments

We thank *M. Barsdell* for kindly providing samples from Merelava and western Epi samples, Dr. *G. Wheller* for Bali samples, and Dr. *S. Eggins* for Ambrym samples. We also thank Mr. *W. Jablonski* for his assistance with microprobe analyses and mapping. *G. Yaxley* generously provided some unpublished results. We thank Prof. *D. H. Green*, *I. Sigurdsson*, *G. Yaxley*, and Dr. *L. Danyushevsky* for fruitful comments and discussions. This paper was written while *M. Gasparon* and *F. N. Della-Pasqua* were PhD students at the University of Tasmania in receipt of a "University of Tasmania Postgraduate Research Award", and an "Australian Postgraduate Research Award" scholarships respectively. The reviewers are thanked for constructive criticism.

References

Allan JF, Sack RO, Batiza R (1988) Cr-rich spinels as petrogenetic indicators: MORB-type lavas from the Lamont seamount chain, eastern Pacific. Am Mineral 73: 741–753

Aoki K (1968) Petrogenesis of ultrabasic and basic inclusions in alkali basalts, Iki Island, Japan. Am Mineral 53: 241–256

Aoki K, Shiba (1973) Pyroxene from lherzolites inclusions from Itinome-gata, Japan. Lithos 6: 41–51

Aoki K, Prinz M (1974) Chromian spinels in lherzolite inclusions from Itinome-gata, Japan. Contrib Mineral Petrol 46: 249–256

Arai S (1987) An estimation of the least depleted spinel peridotite on the basis of olivine-spinel mantle array. N Jb Miner Mh 8: 347–354

Arai S (1992) Chemistry of chromian spinel in volcanic rocks as a potential guide to magma chemistry. Mineral Mag 56: 173–184

Arculus RJ (1974) Solid solution characteristics of spinels: pleonaste-chromite-magnetite compositions in some island-arc basalts. Carnegie Inst Wash Year Book 73: 322–327

Arculus RJ (1978) Mineralogy and petrology of Grenada, Lesser Antilles island arc. Contrib Mineral Petrol 65: 413–424

Arculus RJ, Wills KJA (1980) The petrology of plutonic blocks and inclusions from the Lesser Antilles island arc. J Petrol 21: 743–799

Barsdell M (1988) Petrology and petrogenesis of clinopyroxene-rich tholeiitic lavas, Merelava volcano, Vanuatu. J Petrol 29: 927–964

Barsdell M, Berry RF (1990) Origin and evolution of primitive island arc ankaramites from Western Epi, Vanuatu. J Petrol 31: 747–777

Bartels KS, Kinzler RJ, Grove TL (1991) High pressure phase relations of primitive high-alumina basalts from Medicine Lake volcano, northern California. Contrib Mineral Petrol 108: 253–270

Binns RA (1969) High-pressure megacrysts in basaltic lavas near Armidale, New South Wales. Am J Sci 267-A: 132–168

Binns RA, Duggan MB, Wilkinson JFK (1970) High-pressure megacrysts in alkaline lavas from northeastern New South Wales. Am J Sci 269: 132–168

Bissainte M, Hernandez J, Semet MP, Boudon G (1993) Al-bearing parageneses in the lavas and cumulates from the Monts Caraibes (South Guadeloupe—West Indies). Abstract IAVCEI 1993 Ancient volcanism and modern analogues. General assembly Canberra, Australia, pp 10

Cameron KL, Papike JJ, Bence A, Sueno S (1973) Petrology of fine-grained rock fragments and petrologic implications of single crystals from the Luna 20 soil. Geochim Cosmochim Acta 37: 775–793

Crawford AJ (1980) A clinoenstatite-bearing cumulate olivine pyroxenite from Howqua, Victoria. Contrib Mineral Petrol 75: 353–367

Crawford AJ, Greene HG, Exon NE (1988) Geology, petrology and geochemistry of submarine volcanoes around Epi island, New Hebrides island arc. In: *Greene HG, Wong FL* (eds) Geology and offshore resources of Pacific island arcs—Vanuatu region. Circum-Pacific Council for Energy and Mineral Resources; Earth Science Series 8: 301–327

DeBari SM, Coleman RG (1989) Examination of the deep levels of an island arc: evidence from the Tonsina ultramafic-mafic assemblage, Tonsina, Alaska. J Geophys Res 94: 4373–4391

DeBari SM, Kay SM, Kay RW (1987) Ultramafic xenoliths from Adagdak Volcano, Adak, Aleutian Islands, Alaska: deformed igneous cumulates from the Moho of an island arc. J Geol 95: 329–341

Delano JM (1980) Chemistry and liquidus phase relations of Apollo 15 red glass: implications for the deep lunar interior. Proc 11 Lunar Planet Sci Conf, pp 251–288

Dick HJB, Bryan WB (1978) Variation of basalt phenocryst mineralogy and rock compositions in DSDP hole 396B. In: *Dimitriev L, Heirtzler R*, et al (eds) Init Rept, DSDP, 46: 215–226 (Washington, US Govt Printing Office)

Dick H, Bullen T (1984) Chromian spinel as a petrogenetic indicator in abyssal and alpine-type peridotites and spatially associated lavas. Contrib Mineral Petrol 86: 54–76

Dick HJB, Fisher RL (1984) Mineralogical studies of the residues of mantle melting: abyssal and alpine-type peridotites. In: Kornprobst J (ed) Kimberlites II: the mantle and crust-mantle relationships. Proc Third Inter Kimberlite Conf. Elsevier, Amsterdam, pp 295–308

Drever HI, Johnston R, Gibb FGF (1972) Chromian pleonaste and aluminous picotite in two Apollo 14 microbreccias 14306 and 14055. Nature 235: 30–31

Droop GRT, Bucher-Nurminen K (1984) Reaction textures and metamorphic evolution of sapphirine-bearing granulites from the Gruf Complex, Italian Central Alps. J Petrol 25: 766–803

Eggins S (1989) The origin of primitive ocean island and island arc basalts. Thesis, University of Tasmania, pp 402

Exley RA, Smith JV (1983) Alremite, garnetite and eclogite xenoliths from Bellsbank and Jagersfontein, South Africa. Am Mineral 68: 512–516

Falloon TJ, Green DH (1987) Anhydrous partial melting of MORB pyrolite and other peridotite compositions at 10 Kbar; implications for the origin of primitive MORB glasses. Mineral Petrol 37: 181–219

Fan Q, Hooper PR (1989) The mineral chemistry of ultramafic xenoliths of Eastern China: implications for upper mantle compositions and the paleogeotherms. J Geol 30: 1117–1158

Finger LW (1972) The uncertainty in the calculated ferric iron content of a microprobe analysis. Carnegie Inst Wash Year Book 71: 600–603

Fisk MR, Bence AE (1980) Experimental crystallisation of chrome spinel in FAMOUS basalt 527-1-1. Earth Planet Sci Lett 48: 111–123

Frezzotti ML, De Vivo B, Clocchiatti R (1991) Melt-mineral-fluid interaction in ultramafic nodules from alkaline lavas of Mount Etna (Sicily, Italy): melt and fluid inclusion evidence. J Volcanol Geotherm Res 47: 209–219

Gasparon M (1993) Origin and evolution of mafic volcanics of Sumatra (Indonesia): their mantle source, and the roles of subducted oceanic sediments and crustal contamination. Thesis, University of Tasmania, pp 395

Graham IJ (1987) Petrography and origin of metasedimentary xenoliths in lavas from Tongariro volcanic centre. New Zealand J Geol Geophys 30: 139–157

Grapes RH (1986) Melting and thermal reconstitution of pelitic xenoliths, Wehr volcano, East Eifel, West Germany. J Petrol 27: 343–396

Green DH, Ringwood AE, Ware NG, Hibbersson WO (1972) Experimental petrology and petrogenesis of Apollo 14 basalts. Proc Third Lunar Sci Conf, pp 179–206

Green TH (1992) Petrology and geochemistry of basaltic rocks from the Balleny Is, Antarctica. Aust J Earth Sci 39: 603–617

Griffin WL, Wass SY, Hollis JD (1984) Ultramafic xenoliths from Bullenmerri and Gnotuk Maars, Victoria, Australia: petrology of a sub-continental crust-mantle transition. J Petrol 25: 53–87

Haggerty SE (1972) Subsolidus reaction and compositional variations of spinel. In: *King EA Jr* (ed) Proc Third Lunar Sci Conf, pp 305–332

Hamlyn PR (1975) Chromite alteration in the Panton Sill, East Kimberly region, Western Australia. Mineral Mag 40: 181–192

Holloway JR (1973) The system pargasite-H_2O–CO_2: a model for the melting of a hydrous mineral with a mixed-volatile fluid-I. Experimental results to 8 Kbar. Geochim Cosmochim Acta 37: 651–666

Horning I, Wörner C (1992) Zirconolite bearing ultra-potassic veins in a mantle-xenolith from Mt Melbourne volcanic field, Victoria Land, Antarctica. Contrib Mineral Petrol 106: 355–366

Imsland P (1980) The petrology of the volcanic island Jan Mayen, Arctic Ocean. Nordic Volcanological Institute, University of Iceland, 501p

Irvine TN (1965) Chromian spinel as a petrogenetic indicator, part 1. Theory. Can J Earth Sci 2: 648–672

Irvine TN (1967) Chromian spinel as a petrogenetic indicator, part 2. Petrological applications. Can J Earth Sci 4: 71–103

Jaques AL, Chappell BW, Taylor SR (1983) Geochemistry of cumulus peridotites and gabbros from the Marum Ophiolite Complex, northern Papua New Gunea. Contrib Mineral Petrol 83: 154–164

Jaques AL, Foley SF (1985) The origin of Al-rich spinel inclusions in leucite from the leucite lamproites of Western Australia. Am Mineral 70: 1143–1150

Jarosewich EL, Nelen JA, Norberg JA (1980) Reference samples for electron microprobe analysis. Geostandards Newsletter 4: 43–47

Johnston AD, Draper DS (1992) Near-liquidus phase relations of an anhydrous high-magnesia basalt from the Aleutian Islands: implications for arc magma genesis and ascent. J Volcanol Geotherm Res 52: 27–41

Kay SM, Snedden WT, Foster BP, Kay RW (1983) Upper mantle and crustal fragments in the Ithaca kimberlites. J Geol 91: 277–290

Keil K, Bunch TE, Prinz M (1970) Mineralogy and compositions of Apollo 11 Lunar samples. In: *Levinson AA* (ed) Proc Apollo 11 Lunar Sci Conf. Pergamon, New York, pp 561–598

Kuehener SM, Edgar AD, Arima M (1981) Petrogenesis of the ultrapotassic rocks from the Leucite Hills, Wyoming. Am Mineral 66: 663–677

Kushiro I (1960) Si–Al relation in clinopyroxenes from igneous rocks. Am J Sci 258: 548–554

Kushiro I (1987) A petrological model of the mantle wedge and lower crust in the Japanese island arcs. In: *Mysen BO* (ed) Magmatic processes: physicochemical principles. Geochemical Society, Spec Publ No 1, pp 165–181

Kushiro I (1990) Partial melting of mantle wedge and evolution of island arc crust. J Geophys Res 95: 15929–15939

Kushiro I, Yoder HS (1966) Anorthite-forsterite and anorthite-enstatite relations and their bearing on the basalt-eclogite transformation. J Petrol 7: 337–362

Lavrentev Y, Pospelova LN, Sobolev NV (1974) Rock-forming mineral composition determinations by X-ray microanalysis. Zavodskaya Laboratoria 40: 657–666

Lykins RL, Jenkins DM (1992) Experimental determination of pargasite stability relations in the presence of orthopyroxene. Contrib Mineral Petrol 112: 405–413

Maurel C, Maurel P (1982) Etude experimentale de la distribution de l'aluminium entre bain silicate basique et spinelle chromifere. Implications petrogenetiques: teneur en chrome des spinelles. Bull Minéral 105: 197–202

Maurel C, Maurel P (1983) Influence du fer ferrique sur la distribution de l'aluminium entre bain silicaté basique et spinelle chromifère. Bull Minéral 106: 623–624

Mazzone P, Haggerty SE (1986) Corganites and corgaspinites: two new types of aluminous assemblages from the Jagersfontein kimberlite pipe. Proc Fourth Inter Kimberlite Conf, pp 795–808

Neal CR, Nixon PH (1985) Spinel-garnet relationships in mantle xenoliths from the Malaita alnoites, Solomon islands, South-western Pacific. Trans Geol Soc S Afr 88: 347–354

Nielsen RL, Dungan MA (1983) Low pressure mineral-melt equilibria in natural anhydrous mafic systems. Contrib Mineral Petrol 84: 310–326

Nixon PH, Chapman NA, Gurney JJ (1978) Pyrope-spinel (alkremite) xenoliths from kimberlite. Contrib Mineral Petrol 65: 341–346

Obata M (1980) The Ronda peridotite: garnet-, spinel-, and plagiclase-lherzolite facies and the P-T trajectories of a high-temperature mantle intrusion. J Petrol 21: 533–572

Pasteris JD (1983) Spinel zonation in the De Beers kimberlite, South Africa: possible role of phlogopite. Can Mineral 21: 41–58

Pearcy LG, DeBari SM, Sleep NH (1990) Mass balance calculations for the formation of continents. Earth Planet Sci Lett 96: 427

Prince GD, Putnis A (1979) Oxidation phenomena in pleonaste bearing titanomagnetites. Contrib Mineral Petrol 69: 355–359

Raheim A, Green DH (1974) Experimental petrology of lunar highland basalt composition and applications to models for the lunar interior. J Geol 82: 607–622

Reid AM, Dawson JB (1972) Olivine-garnet reaction in peridotites from Tanzania. Lithos 5: 115–124

Reid AM, Donaldson CH, Dawson RW, Brown RW (1975) The Igwisi Hills extrusive "Kimberlites". Phys Chem Earth 9: 199–218

Reid AM, Ridley WI, Harmon RS, Warner J, Brett R (1972) Highly aluminous glasses in lunar soils and the nature of the lunar highlands. Geochim Cosmochim Acta 36: 903–912

Reid JB (1972) Olivine-rich, true spinel—bearing anorthosites from Apollo 15 & Luna 20 soils—possible fragments of the earliest formed lunar crust. In: *Chamberlain JW , Watkins C* (eds) The Apollo 15 Lunar samples. Lunar Science Institute, Houston, pp 154–157

Roeder E, Weiblen PW (1972) Occurrence of chromian, hercynitic spinel ("pleonaste") in Apollo-14 samples and its petrologic implications. Earth Planet Sci Lett 15: 376–402

Roeder PL, Reynolds I (1991) Crystallisation of chromite and chromium solubility in basaltic melts. J Petrol 32: 909–934

Romick JD, Perfit MR, Swanson SE, Shuster RD (1990) Magmatism in the eastern Aleutian arc: temporal characteristics of igneous activity on Akutan island. Contrib Mineral Petrol 104: 700–721

Sack RO, Ghiorso MS (1991) Chromian spinels as petrogenetic indicators: thermodynamics and petrological applications. Am Mineral 76: 827–847

Schreiber HD, Haskin LA (1976) Chromium in basalts: experimental determination of redox states and partitioning among synthetic silicate phases. Proc 7th Lunar Sci Conf, pp 1221–1259

Sen G, Leeman W (1991) Iron-rich lherzolitic xenoliths from Oahu: origin and implications for Hawaiian magma sources. Earth Planet Sci Lett 102: 45–57

Sigurdsson H (1977) Spinels in leg 37 basalts and peridotites: phase chemistry and zoning. Init Repts DSDP 37: 883–891

Sigurdsson H, Schilling JG (1976) Spinels in Mid-Atlantic ridge basalts: chemistry and occurrence. Earth Planet Sci Lett 29: 7–20

Snoke AW, Quick JE, Bowman HR (1981) Bear Mountain igneous complex, Klamath Mountains, California: an ultrabasic to silicic calc-alkaline suite. J Petrol 22: 501–552

Sobolev AV, Dmitriev LV, Barsukov VL, Nevsorov VN, Slutsky AB (1980) The formation conditions of the high-magnesium olivines from monomineralic fraction of Luna 24 regolith. Proc 11th Lunar Planet Sci Conf. Pergamon Press, New York, pp 105–116

Talbot JL, Hobbs B, Wilshire HG, Sweatman TR (1963) Xenoliths and xenocrysts from lavas of the Kerguelen Archipelago. Am Mineral 48: 159–179

Thy P (1991) High and low pressure phase equilibria of a mildly alkalic lava from the 1965 Surtsey eruption: experimental results. Lithos 26: 223–243

van Bemmelen RW (1949) The geology of Indonesia. Government Printing Office, The Hague

Varne R (1977) On the origin of spinel iherzolite inclusions in basaltic rocks from Tasmania and elsewhere. J Petrol 18: 1–23

Venturelli G, Capedri S, Di Battistini G, Crawford A, Kogarko LN, Celestini S (1984) The ultrapotassic rocks from southeastern Spain. Lithos 17: 37–54

Wagner C, Velde D (1987) Aluminous spinels in lamproites: occurrence and probable significance. Am Mineral 72: 689–696

Walker DA, Cameron WE (1983) Boninite primary magmas: evidence from Cape Vogel peninsula, Papua New Guinea. Contrib Mineral Petrol 83: 150–158

Wass SY (1973) Plagioclase-spinel intergrowths in alkali basaltic rocks from the Southern Highlands, N.S.W. Contrib Mineral Petrol 38: 167–175

Weibe RA (1986) Lower crustal cumulate nodules in Proterozoic dikes of the Nain Complex: evidence for the origin of Proterozoic anorthosites. J Petrol 27: 1253–1275

Wheller GE (1986) Petrogenesis of Batur caldera, Bali, and the geochemistry of Sunda-Banda arc basalts. Thesis, University of Tasmania, pp 156

Wilkinson JFK (1973) Pyroxenite xenoliths from an alkali trachybasalt in the Glen Innes area, northeastern New South Wales. Contrib Mineral Petrol 42: 15–32

Wilkinson JFK (1975) An Al-spinel ultramafic-mafic inclusion suite and high pressure megacrysts in an analcimite and their bearing on basaltic magma fractionation at elevated pressures. Contrib Mineral Petrol 53: 71–104

Yaxley GM, Crawford AJ, Green DH (1991) Evidence for carbonatite metasomatism in spinels peridotite xenoliths from western Victoria, Australia. Earth Planet Sci Lett 107: 305–317

Yim WWS (1990) Heavy mineral provenance and the genesis of stanniferous placers in northeastern Tasmania. Thesis, University of Tasmania, pp 303

Author's address: *F. N. Della-Pasqua*, Department of Geology, University of Tasmania, GPO Box 252C, Hobart, Tasmania 7001, Australia